Flue gas purification with membranes based on the polymer of intrinsic microporosity PIM-TMN-Trip

Flue gas purification with membranes based on the polymer of intrinsic microporosity PIM-TMN-Trip

Petr Stanovsky[1], Andrea Zitkova[1], Magda Karaszova[1], Michal Šyc[1], Johannes Carolus Jansen[2], Bibiana Comesaña Gándara[3], Neil McKeown[3], Pavel Izak[1,4,*]

[1]The Czech Academy of Sciences, Institute of Chemical Process Fundamentals, Rozvojova 135, 165 02 Prague 6 – Suchdol, Czech Republic

[2] Institute on Membrane Technology, ITM-CNR, Via P. Bucci 17/C, 87036 Rende (CS), Italy

[3] EaStCHEM School of Chemistry, University of Edinburgh, David Brewster Road, Edinburgh EH9 3FJ, Midlothian, Scotland

[4] MemBrain s.r.o., Pod Vinicí 87, 471 27 Stráž pod Ralskem, Czech Republic

* corresponding author: izak@icpf.cas.cz

Abstract

Flue gas purification experiments were performed with a membrane made from the ultrapermeable polymer of intrinsic microporosity (PIM) based on tetramethyltetrahydronaphthalene unit coupled with bicyclic triptycene (PIM-TMN-Trip). Permeation experiments with a CO_2-N_2-O_2-SO_2 mixture, simulating flue gas from power plants, were performed by means of an in-house developed permeation unit. The results showed very high permeability of the membrane for sulfur dioxide SO_2 and high permeability of CO_2, lying mainly between the Robeson upper bound form 2008 and the recently reported upper bound from 2019. Moderately high mixed gas selectivity of SO_2 and CO_2 with respect to N_2 (21-29 and 11-18, respectively), in combination with very high permeability ($28 \cdot 10^3$ and $30 \cdot 10^3$ Barrer, respetively), suggest potential use for industrial gas separation processes. The SO_2/CO_2 mixed gas selectivity was relatively low (around 1.8), but comparable with other novel membranes, and both are removed simultaneously in the process of CO_2 separation.

Keywords

flue gas purification, gas permeation, polymer of intrinsic microporosity, membrane gas separation

1   Introduction

Fossil fuels combustion is still world's leading method for heat and power generation and this process is a large source of carbon dioxide as well as sulfur dioxide emissions [1]. There are

also other sources of CO_2 and SO_2 emissions from the industrial production of metals, glass, cement, ceramics or from waste incineration. In the case of SO_2, there are already established technologies for elimination of its emissions to legislative limits, however the used technologies consume a large amount of natural resources, such as lime, limestone, trona, etc. Furthermore, emission limits are gradually decreasing and other technologies are likely needed in the future. On the other hand, the technology for the capture of the greenhouse gas CO_2 is currently being developed but it is not fully mature and there is call to increase effort in the development of this technology, especially in Europe [2, 3]. Intensive research on membranes for either CO_2 removal from flue gas streams or upgrading of gas effluents for energy production based on renewable sources over last decade due led to significant increase of membrane transport and separation properties [3, 4]. However, more permeable and durable materials for CO_2 separation are needed to make these technologies more profitable and economically competitive [5]. There are only several commercial membrane modules generally used for flue gas separation that have been tested under real conditions with flue gas at pilot scale with different results [6-10]. The most successful seem to be the Polaris™ membrane produced by MTR [10], which, with its CO_2 permeance of 2000 GPU and CO_2/N_2 selectivity of 50, defined the new optimum of membrane transport properties for CO_2 removal from flue gas, and is used as an example in optimization studies [11-16]. These studies indicate that a really large membrane area will be required if we want to avoid additional compression of the flue gas. That is why the effort of many research teams is still put into the development of membrane materials with better transport properties, in particular higher permeability. There are several promising new directions in membrane science for gas separation, such as the use of mixed-matrix membranes, or ionic liquid supported membranes, aiming to improve their separation performance and transport properties [17, 18]. For the homogenous polymeric materials, it has been suggested by theoretical analysis that successful membranes need to be based on rigid polymers [19]: "(polymer) *backbone stiffness increases should be coupled with increases in interchain separation to achieve both higher permeability and higher selectivity*". The relatively new class of so-called polymers of intrinsic microporosity (PIM) seems to fulfill this perfectly [20, 21]. PIM's owe their superb separation performance and transport properties to the inefficiently packed two-dimensional chains and their contorted three-dimensional conformation, using different structural elements such as benzotriptycene, spirobifluorene, Tröger's base, etc. [21-26]

In this work we report the performance of one of these promising materials, PIM-TMN-Trip [21] with a mixture of gases reflecting the composition of flue gas produced by coal power plants. The scope of this work is to test the performance of this polymer, that has recently been used to re-define the upper bound for CO_2/CH_4 and CO_2/N_2 for pure gases [27], with a synthetic flue gas mixture containing traces of SO_2. The final aim is to evaluate the efficiency of SO_2 removal from the flue gas, and the possible separation of SO_2 from CO_2.

2   Experimental

2.1 Materials and membrane preparation

The synthesis of PIM-TMN-Trip (Fig. 1) is described in detail by Rose et al. [21].The PIM-TMN-Trip membranes were prepared from a 10 wt. % polymer solution in chloroform which was filtered through a 3.1 μm glass-fiber syringe filter to remove dust and insoluble polymer traces, degassed at room temperature and finally cast onto a well-leveled Petri dish. Then, the solvent was allowed to evaporate at room temperature over a period of 96 – 120 h, until the membranes detached spontaneously from its glass support, slowing down the evaporation by partially covering the Petri dish. Afterwards, the self-supported membranes were soaked in fresh methanol to remove residual casting solvent and finally dried in the air over a period of 24 h.
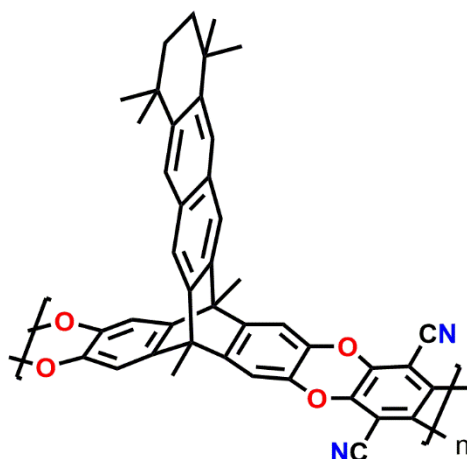

Fig. 1. Chemical structure of PIM-TMN-Trip polymer

All gases except air were purchased from LindeGas. Air was supplied from institutional clean air supply and its cleanness was further assured through a set of filters Kaeser, type FC-18B a FF-18B and a Julabo cooling bath set up to 3°C. The gas mixtures for the permeability measurements were prepared by in-line mixing of pure CO_2 (99.95%) and N_2 (99.996%) in the desired ratios. Further tests were performed with a mixture of CO_2 and SO_2-containing N_2 (with a certified concentration of 5000 ppm SO_2 in N_2 as the calibrated gas for analytical purposes), that was further diluted with pure N_2 (99.996%) to reduce the SO_2 concentration to the desired level.

2.2 Membrane characterization

Scanning Electron Microscopic (SEM) analysis of the samples was performed on a Tescan Vega3 electron microscope at an acceleration voltage of 15 kV. The samples were freeze-fractured in liquid nitrogen for analysis of the cross-section and the samples were sputtered with gold before analysis.

The thickness of the membranes was determined using a digital micrometer (Micromaster Capaμsystem IP54, Switzerland) as the average of ten measurements over the entire membrane area used during the permeability measurements.

2.3 *Permability measurements*

The gas permeation experiments of selected gases and gas mixtures were carried out using a custom-made continuous flow permeation apparatus (designed and constructed at ICPF). The apparatus is controlled via National Instruments analog/digital I/O boards and operated via routines programmed in LabVIEW to control the pressure and to the the gas composition. The exposed membrane area was 15.91 cm^2 and the average thickness was 161±13 micrometers. The gas permeation rig, depicted in Fig. 2, allows setting of the SO_2 concentration in the feed stream mixture of N_2, CO_2 and air at a given pressure and relative humidity.
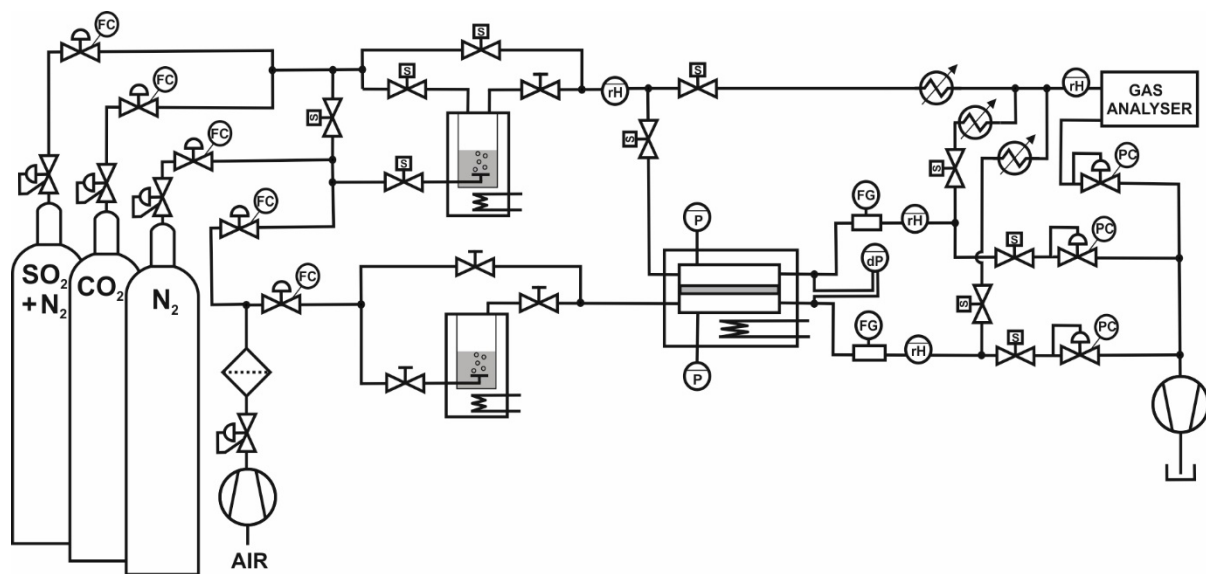

Fig. 2. Scheme of the $N_2/SO_2/CO_2$ permeation apparatus with humidity control. FC - flow controllers, P – pressure gauges, FG – flow gauges, rH – humidity gauges, PC – pressure controllers, S – electromagnetic valves.

The sweep stream can be either pure N_2 or air. Both input streams have controlled humidity by means of a thermostated saturator, and humidity is measured for the feed, permeate and retentate streams (HygroFlex 4 system with HC2 sensors). A set of flow controllers (Bronkhorst El-Flow Select, range 3-100 ml min^{-1}) controls the final feed composition and the flow rate of the feed and the sweep stream. After the thermostated membrane cell, a set of electromagnetic valves allows to analyze either the retentate or the permeate stream in the analyzer, working with set of electrochemical and infrared detectors (ASEKO AIR LAB). Flow gauges based on gas thermal mass flow measurement characterize both output streams (Bronkhorst El-Flow Select, range 6-125 ml min^{-1}). The upper side of the membrane cell can be set to higher pressure with a backward-operating pressure controller (Bronkhorst El-Press, range 25-500 kPa). The permeate and sweep stream is working at atmospheric pressure or slightly lower than atmospheric pressure, and is controlled by backward-operating pressure

controller (Bronkhorst, range 5-100 kPa), but it can be also be set to low vacuum, although this option does not allow to analyze the permeate stream directly. Humidity from all streams is removed before the gas analyzer by means of a freezing trap, because water vapor has an adsorption band at a similar wavelength as the operating range of the infrared SO_2 analyzer. All equipment is built inside a termostated box, where the temperature is controlled with an accuracy of $\pm$ 0.2°C. Before each set of measurements, the calibration of the SO_2 sensor was checked in the measurement range of 0-2500 ppm.

In this study, membranes were tested with a feed mixture containing 2220 ppm of SO_2 in 22.2 vol% of CO_2, and rest of mixture was 6.8 vol% of O_2 and 70.2 vol% N_2. The upstream pressure was changed over the range from 200 to 500 kPa and the downstream pressure was kept at 90 kPa. The feed flow was set to 50 ml min^{-1} and the sweep flow was air with a flow rate of 30 ml min^{-1}. The temperature of both streams was set to 25 °C.

2.4 Calculations

The permeability is this work was evaluated according relation:

$$P_i = \frac{J_i\,l}{\Delta p_m},$$

Eq. 1

where J_i is permeation flux of the particular gas i through the membrane at steady state, l is the thickness of the membrane and Δp_m is the driving force, *i.e.* the partial pressure difference of gas i between feed and permeate. As the streams in the membrane cell flow radially along the circular membrane from its center to its edges in concurrent arrangement, the logarithmic average of the partial pressure of respective streams must be used and the driving force is calculated according to the following formula

$$\Delta p_m = \frac{(p_i^{feed} - p_i^{perm}) - (p_i^{ret} - p_i^{sweep})}{\ln(p_i^{feed} - p_i^{perm}) - \ln(p_i^{ret} - p_i^{sweep})}\,,$$

Eq. 2

The selectivity was calculated as the ratio of the permeabilities of the gas pairs i and j:

$$\alpha_{i/j} = {P_i}\big/{P_j},$$

Eq. 3

where P is expressed in the unit *Barrer*, recalculated from SI units, as:

$$1\ Barrer = 3.35 \cdot 10^{-16}\frac{mol}{m.s.Pa}.$$

3   Results and discussion

The PIM-TMN-Trip membrane was tested for the separation of SO_2 and CO_2 from a feed stream containing of 22 vol% of CO_2 and 2220 ppm of SO_2 in air with air as the sweeping gas, resembling one of the possible configurations for industrial flue gas cleaning. The gas separation tests were performed at a relatively low pressure because energy requirements would be higher due to the necessary compression of the feed, although the required membrane area would be proportionally much smaller.

The membrane was tested for a total of one month, during which changes in the thickness or in the size size due to swelling were not observed. A SEM image of the membrane structure in the cross-section is shown in Fig. 3.
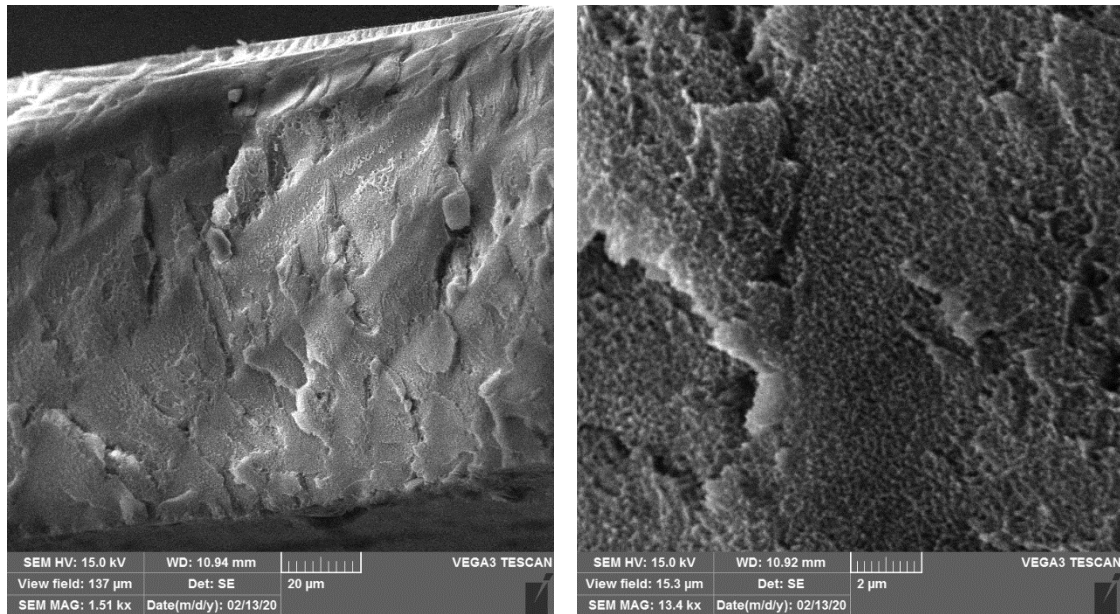

Fig. 3. SEM image of the membrane cross-section after the gas permeation experiments.

The surface on the left image shows the typical morphology of a brittle fracture, what is especially apparent in the right image with 9x higher magnification (13,400 x). This behavior can indeed be expected for glassy polymers like PIMs. The image further shows a dense structure, confirming that PIM-TMN-Trip was not compromised by the repeated pressure changes (due to the use of trans-membrane pressure differences up to 400kPa). During the various measurement cycles, the structure remained dense and without the formation of internal voids or surface cracks.

In the permeation tests with the model flue gas, the permeability of SO_2 and CO_2 remain almost constant with increasing feed pressure or trans-membrane pressure difference (Fig. 4A).
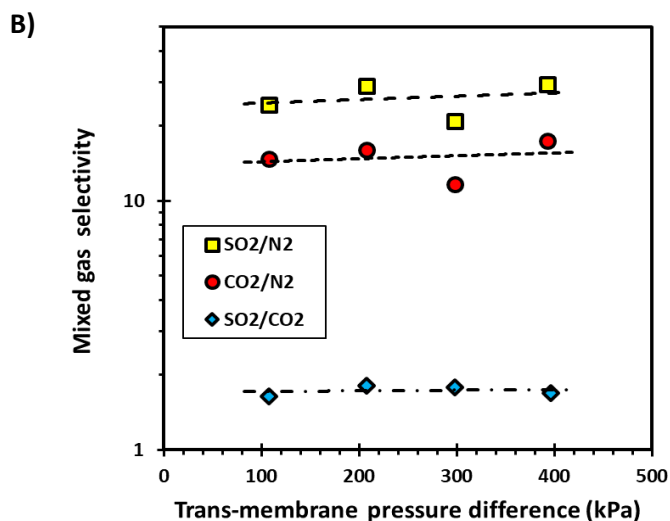
B)
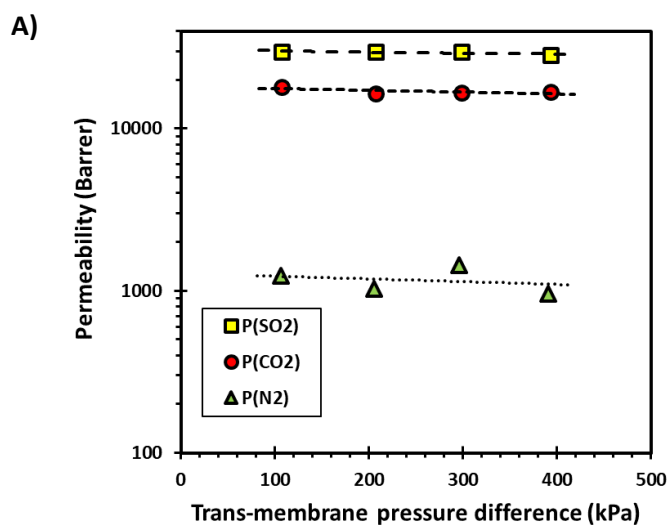
Fig. 4. Mixed gas permeability (A, top) and selectivities (B, bottom) for a synthetic flue gas mixture of SO_2 and CO_2 in air (2220 ppm SO_2 in a mixture of 22% CO_2 and 78% air, feed flow rate 50 ml min^{-1}, sweep flow rate 30 ml min^{-1}). Trendlines are plotted as a guide to the eye.

The permeability of SO_2 ranges from 29900 Barrer to 28300 Barrer. The permeability of CO_2 is lower than that of SO_2 and ranges from 18200 Barrer to 16500 Barrer. Independence of permeability with respect to changes of the feed pressure indicates that the transport of these gases in the membrane obeys the diffusion-solution model despite of the high stage cut for both desired compounds, as can be seen in Fig. 4. The higher permeability of SO_2 than CO_2 should most likely be attributed to the higher solubility of SO_2 in the polymer. Since the kinetic diameter of SO_2 (0.36 nm) is slightly larger than that of CO_2 (0.33 nm) [28], and since these polymers were found to be highly size selective [29], the diffusion coefficient of SO_2 is expected to be considerably lower than that of CO_2. The permeability of SO_2 is therefore so high, mostly due to its strong affinity to the polymer because with its relatively high molar mass with and its permanent dipole moment, SO_2 should be much more condensable gas in comparison to CO_2 or other gases in the mixture. Indeed, the critical temperature of SO_2 (157.5 °C), is much higher than that of CO_2 (31 °C), which is an indication of a much stronger condensability of SO_2. The resulting SO_2/CO_2 mixed gas selectivity is almost independent on the trans-membrane pressure difference, as can be seen on Fig. |4B, and its value is rather low ~1.8, which means that they are not easily separated, one from the other, but both can be efficiently removed from air. Mixed gas selectivities for SO_2/N_2 and CO_2/N_2 slightly vary with increasing trans-membrane pressure difference but their values (12-18 and 21-30, respectively) are sufficiently high for industrially relevant separations. Only water vapor usually present in flue gas could be competitive species, as it is more condensable gas than SO_2 [28]. This effect was initially suppressed in our case by using a feed gas and a sweep gas with low relative humidity of about 5%. We did not observe any significant enrichment of the permeate with

humidity or depletion of the retentate, as the maximum change in the output streams was about 2%, which is comparable with the uncertainty of the humidity sensor.

Due to the high permeability of the membranes and the relatively large membrane area, a high stage cut for both gases is achieved, especially at increasing trans-membrane pressure (Fig. 4). A high stage-cut is desirable as the proof that both pollutants can be effectively removed from flue gases. On the other hand, since the testing rig was designed for testing membranes with permeability parameters similar to industrially used membranes for gas separation (e.g. Polaris, etc., with much lower permeance), this ultrapermeable membrane was tested under conditions, in which the measured permeability may be lower than that reported in the literature for pure gases, due to concentration polarization phenomena.
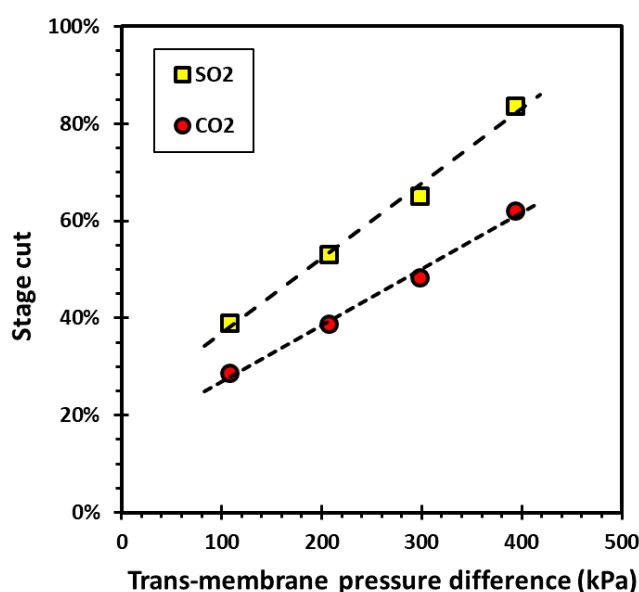

Fig. 5. Stage cut of SO_2 and CO_2 from flue gas at given conditions (2220 ppm SO_2 and 22 vol% CO_2 in the feed, feed flow rate 50 ml min^{-1}, sweep flow rate 30 ml min^{-1}). Trendlines are plotted as a guide to the eye.

Comparison with other polymeric membranes for this gas pair from the literature [28, 30] at Fig. 6 shows that the SO_2/CO_2 selectivity is somewhat lower than that of other membranes, but at much higher SO_2 permeability, thus surpassing the upper bound from the literature [30]. Hence, this membrane is ultrapermeable even for SO_2, which is desirable in flue gas purification. It must be noted that the upper bound in Fig. 6 is derived from theoretical considerations, and is of course not drawn on the basis of the points in the graph itself. Interestingly, the low selectivity for SO_2/CO_2 of PIM-TMN-Trip is comparable with that of thermally rearranged membranes (denoted as TR in Fig. 5), but the SO_2 permeability is almost two orders of magnitude higher in our PIM. The PIM-TMN-Trip membrane has a comparable selectivity as a recently reported water-swollen thin film membrane for separation of SO_2 from similar flue gas mixtures, based on a Toray membrane, but the present PIM has a significantly higher permeability for SO_2 than that reported in the literature [31]. Similarly to the present

PIM, these water-swollen membranes and thermally rearranged membranes have also shown excellent performance for CO_2/CH_4 separation [30, 32-34]. Permeability of SO_2 is so high that one might expect a certain degree of concentration polarization. However, the negative effect on the separation factor may be limited due to the low initial SO_2 concentration in the feed. In any case, the separation factor is also reduced by the high stage-cut under the given conditions.
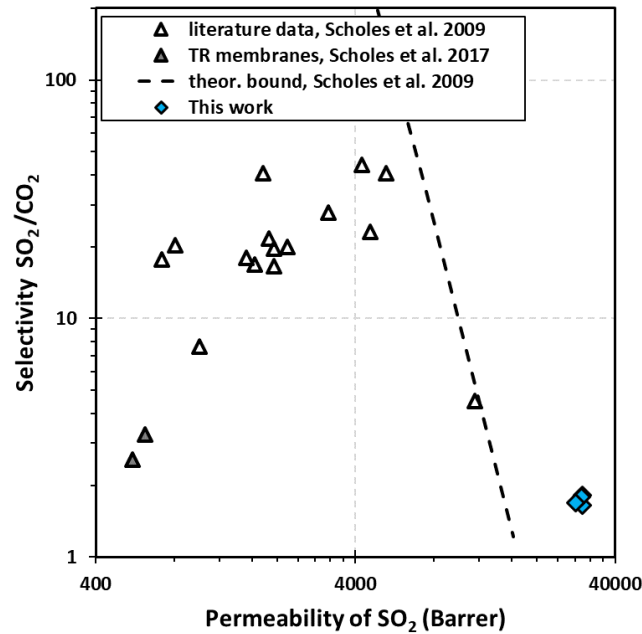

Fig. 6. Robeson diagram for SO_2/CO_2 with literature results for various membranes. The dashed line is the upper bound for the separation of SO_2/CO_2 [30] based on the ideal selectivity; Triangles - ideal selectivity and permeability [28, 30]; diamonds – mixed gas selectivity from this work.

The overview in Fig. 7 shows a somewhat lower permeability of CO_2 in comparison with measurements made for PIM-TMN-Trip by Rose *et al.* [21] and Comesaña-Gándara *et al.* [27], who measured pure gas permeability and ideal gas selectivity. The difference might be due to a negative coupling effect, and, given the high stage-cut, also to concentration polarization phenomena. Nevertheless, despite the lower mixed gas permeability, the performance of PIM-TMN-Trip is still excellent even at mixed gas conditions, with CO_2/N_2 mixed gas selectivity ranging from 11 to 18, positioning the values between the 2008 [35] and 2019 [27] upper bounds.
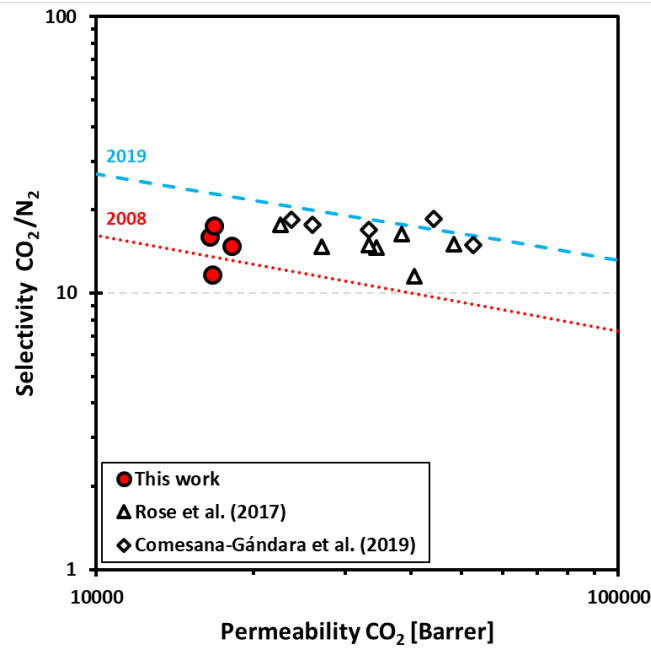
Fig. 7. Trade-off for CO_2/N_2 with experimental results and literature data for PIM-TMN-Trip membrane with different age or processing. Triangles: Rose *et al.* [21]; diamonds: Comesaña-Gándara *et al.* [27]; red circles: mixed gas selectivity and permeability for PIM-TMN-Trip membrane with the model flue gas mixture from this work. Lines are upper bounds for separation of CO_2/N_2 from literature for ideal selectivity: red dotted line: Robeson *et al.* (2008) [35]; blue dashed line: Comesaña-Gándara *et al.* (2019) [27].

For effective SO_2 removal from flue gas streams, the SO_2/N_2 selectivity is the most relevant process parameter. The performance of the tested PIM-TMN-Trip membrane is shown in Fig. 8. The SO_2/N_2 mixed gas selectivity is relatively high, with values ranging from 21 to 29. Comparison with data from literature for ideal selectivity and permeability [36-38] show that much higher selectivity has been reached, but PIM-TMN-Trip outperforms all other membranes in terms of permeability. It must be stressed that previous studies sometimes showed an ambiguous influence of the relative humidity on the membrane permeability of SO_2 [28, 39], and this should be addressed in future studies.
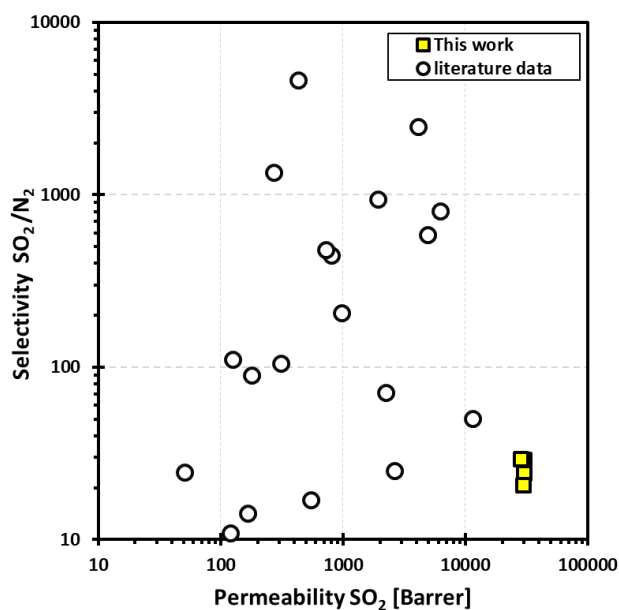
Fig. 9. Robeson-like trade-off diagram between selectivity and permeability for SO_2/N_2 with experimental results for the PIM-TMN-Trip membrane with the synthetic flue gas mixture in this work (yellow squares). Literature data for pure gas permeability and ideal selectivity [36-39] are reported for comparison (white circles).

4   Conclusions

PIM-TMN-Trip membranes show excellent separation properties for CO_2/N_2 as well as for SO_2/N_2. The permeability of CO_2 (with values ranging from $16.5 \cdot 10^3$-$18 \cdot 10^3$ Barrer) was slightly lower than the values reported in literature. However, mixed gas CO_2/N_2 selectivity is at a similar level as the reported ideal selectivity, with trade-off performance values lying in between Robeson's upper bound [35] and recently redefined CO_2/N_2 upper bound for pure gases [27]. The permeability of SO_2 in an air/CO_2 mixture was very high ($28 \cdot 10^3$ -$30 \cdot 10^3$ Barrer) and the SO_2/CO_2 selectivity in this gas mixture was low (around 1.8) but comparable with other novel membranes which have shown good separation properties for CO_2 separation. The effect of pressure on the permeability of CO_2 or SO_2 is minor in the pressure range used in this work. High stage-cut caused by high permeability may lead to concentration polarization phenomena, but this needs to be further studied quantitatively to understand whether the effect of the pressure on the overall separation performance is positive or negative. In any case, the high selectivity of CO_2 and SO_2 in comparison with N_2 in mixed gas separation conditions show promising potential of these membranes for flue gas purification with simultaneous removal of both components.

Acknowledgements

References

[1] OECD/IEA, Electricity generation by fuel - World 1990 - 2016, in, 2019.

[2] Forest bioenergy, carbon capture and storage, and carbon dioxide removal: an update., in: EASAC Reports, European Academies Science Advisory Council, 2019.

[3] E. Esposito, L. Dellamuzia, U. Moretti, A. Fuoco, L. Giorno, J.C. Jansen, Simultaneous production of biomethane and food grade CO2 from biogas: an industrial case study, Energy & Environmental Science, 12 (2019) 281-289.

[4] D.F. Sanders, Z.P. Smith, R. Guo, L.M. Robeson, J.E. McGrath, D.R. Paul, B.D. Freeman, Energy-efficient polymeric gas separation membranes for a sustainable future: A review, Polymer, 54 (2013) 4729-4761.

[5] M.T. Ho, G.W. Allinson, D.E. Wiley, Reducing the cost of CO2 capture from flue gases using membrane technology, Ind Eng Chem Res, 47 (2008) 1562-1568.

[6] T. Brinkmann, J. Lillepärg, H. Notzke, J. Pohlmann, S. Shishatskiy, J. Wind, T. Wolff, Development of CO2 Selective Poly(Ethylene Oxide)-Based Membranes: From Laboratory to Pilot Plant Scale, Engineering, 3 (2017) 485-493.

[7] D. Hasse, J. Ma, S. Kulkarni, P. Terrien, J.-P. Tranier, E. Sanders, T. Chaubey, J. Brumback, CO2 Capture by Cold Membrane Operation, Energy Procedia, 63 (2014) 186-193.

[8] J.P. Montoya, Using Hollow Fiber Membranes to Separate Gases from Liquid and Gaseous Streams, in: Membrane Gas Exchange, MedArray, Inc, 2010.

[9] C.A. Scholes, A. Qader, G.W. Stevens, S.E. Kentish, Membrane pilot plant trials of CO2 separation from flue gas, Greenhouse Gases: Science and Technology, 5 (2015) 229-237.

[10] L.S. White, X.T. Wei, S. Pande, T. Wu, T.C. Merkel, Extended flue gas trials with a membrane-based pilot plant at a one-ton-per-day carbon capture rate, J Membrane Sci, 496 (2015) 48-57.

[11] N.C. Mat, G.G. Lipscomb, Membrane process optimization for carbon capture, International Journal of Greenhouse Gas Control, 62 (2017) 1-12.

[12] T.C. Merkel, H.Q. Lin, X.T. Wei, R. Baker, Power plant post-combustion carbon dioxide capture: An opportunity for membranes, J Membrane Sci, 359 (2010) 126-139.

[13] C. Song, Q. Liu, N. Ji, S. Deng, J. Zhao, Y. Li, Y. Kitamura, Reducing the energy consumption of membrane-cryogenic hybrid CO2 capture by process optimization, Energy, 124 (2017) 29-39.

[14] Y. Wang, L. Zhao, A. Otto, M. Robinius, D. Stolten, A Review of Post-combustion CO2 Capture Technologies from Coal-fired Power Plants, Energy Procedia, 114 (2017) 650-665.

[15] J. Xu, Z. Wang, Z. Qiao, H. Wu, S. Dong, S. Zhao, J. Wang, Post-combustion CO2 capture with membrane process: Practical membrane performance and appropriate pressure, J Membrane Sci, 581 (2019) 195-213.

[16] H. Zhai, Advanced Membranes and Learning Scale Required for Cost-Effective Post-combustion Carbon Capture, iScience, 13 (2019) 440-451.

[17] P. Bernardo, E. Drioli, G. Golemme, Membrane Gas Separation: A Review/State of the Art, Ind Eng Chem Res, 48 (2009) 4638-4663.

[18] X. He, A review of material development in the field of carbon capture and the application of membrane-based processes in power plants and energy-intensive industries, Energy, Sustainability and Society, 8 (2018).

[19] B.D. Freeman, Basis of permeability/selectivity tradeoff relations in polymeric gas separation membranes, Macromolecules, 32 (1999) 375-380.

[20] R. Swaidan, B. Ghanem, I. Pinnau, Fine-Tuned Intrinsically Ultramicroporous Polymers Redefine the Permeability/Selectivity Upper Bounds of Membrane-Based Air and Hydrogen Separations, ACS Macro Letters, 4 (2015) 947-951.

[21] I. Rose, C.G. Bezzu, M. Carta, B. Comesana-Gandara, E. Lasseuguette, M.C. Ferrari, P. Bernardo, G. Clarizia, A. Fuoco, J.C. Jansen, K.E. Hart, T.P. Liyana-Arachchi, C.M. Colina, N.B. McKeown, Polymer ultrapermeability from the inefficient packing of 2D chains, Nat Mater, 16 (2017) 932-937.

[22] J. Benito, J. Vidal, J. Sanchez-Lainez, B. Zornoza, C. Tellez, S. Martin, K.J. Msayib, B. Comesana-Gandara, N.B. McKeown, J. Coronas, I. Gascon, The fabrication of ultrathin films and their gas separation performance from polymers of intrinsic microporosity with two-dimensional (2D) and three-dimensional (3D) chain conformations, J Colloid Interface Sci, 536 (2019) 474-482.

[23] C.G. Bezzu, M. Carta, M.-C. Ferrari, J.C. Jansen, M. Monteleone, E. Esposito, A. Fuoco, K. Hart, T.P. Liyana-Arachchi, C.M. Colina, N.B. McKeown, The synthesis, chain-packing simulation and long-term gas permeability of highly selective spirobifluorene-based polymers of intrinsic microporosity, Journal of Materials Chemistry A, 6 (2018) 10507-10514.

[24] A. Fuoco, B. Comesana-Gandara, M. Longo, E. Esposito, M. Monteleone, I. Rose, C.G. Bezzu, M. Carta, N.B. McKeown, J.C. Jansen, Temperature Dependence of Gas Permeation and Diffusion in Triptycene-Based Ultrapermeable Polymers of Intrinsic Microporosity, ACS Appl Mater Interfaces, 10 (2018) 36475-36482.

[25] I. Rose, M. Carta, R. Malpass-Evans, M.-C. Ferrari, P. Bernardo, G. Clarizia, J.C. Jansen, N.B. McKeown, Highly Permeable Benzotriptycene-Based Polymer of Intrinsic Microporosity, ACS Macro Letters, 4 (2015) 912-915.

[26] R. Swaidan, M. Al-Saeedi, B. Ghanem, E. Litwiller, I. Pinnau, Rational Design of Intrinsically Ultramicroporous Polyimides Containing Bridgehead-Substituted Triptycene for Highly Selective and Permeable Gas Separation Membranes, Macromolecules, 47 (2014) 5104-5114.

[27] B. Comesaña-Gándara, J. Chen, C.G. Bezzu, M. Carta, I. Rose, M.-C. Ferrari, E. Esposito, A. Fuoco, J.C. Jansen, N.B. McKeown, Redefining the Robeson upper bounds for CO2/CH4 and CO2/N2 separations using a series of ultrapermeable benzotriptycene-based polymers of intrinsic microporosity, Energy & Environmental Science, (2019).

[28] C. Scholes, S. Kentish, G. Stevens, Effects of Minor Components in Carbon Dioxide Capture Using Polymeric Gas Separation Membranes, Sep Purif Rev, 38 (2009) 1-44.

[29] A. Fuoco, C. Rizzuto, E. Tocci, M. Monteleone, E. Esposito, P.M. Budd, M. Carta, B. Comesaña-Gándara, N.B. McKeown, J.C. Jansen, The origin of size-selective gas transport through polymers of intrinsic microporosity, Journal of Materials Chemistry A, 7 (2019) 20121-20126.

[30] C.A. Scholes, G. Dong, J.S. Kim, H.J. Jo, J. Lee, Y.M. Lee, Permeation and separation of SO2 , H2S and CO2 through thermally rearranged (TR) polymeric membranes, Separation and Purification Technology, 179 (2017) 449-454.

[31] A. Žitková, M. Kárászová, P. Stanovský, J. Vejražka, P. Izák, Application of Water-Swollen Thin-Film Composite Membrane in Flue Gas Purification, Chem Eng Technol, 42 (2019) 1304-1309.

[32] M. Karaszova, J. Vejrazka, V. Vesely, K. Friess, A. Randova, V. Hejtmanek, L. Brabec, P. Izak, A water-swollen thin film composite membrane for effective upgrading of raw biogas by methane, Separation and Purification Technology, 89 (2012) 212-216.

[33] Z. Sedlakova, M. Karaszova, J. Vejrazka, L. Moravkova, E. Esposito, A. Fuoco, J.C. Jansen, P. Izak, Biomethane Production from Biogas by Separation Using Thin-Film Composite Membranes, Chem Eng Technol, 40 (2017) 821-828.

[34] M. Simcik, M.C. Ruzicka, M. Karaszova, Z. Sedlakova, J. Vejrazka, M. Vesely, P. Capek, K. Friess, P. Izak, Polyamide thin-film composite membranes for potential raw biogas purification: Experiments and modeling, Separation and Purification Technology, 167 (2016) 163-173.

[35] L.M. Robeson, The upper bound revisited, J Membrane Sci, 320 (2008) 390-400.

[36] Y.I. Dytnerskii, G.G. Kagramanov, I.P. Storozhuk, N.F. Kovalenko, SO2 Separation from gaseous mixtures by membranes, J Membrane Sci, 41 (1989) 49-54.

[37] D.L. Kuehne, S.K. Friedlander, Selective Transport of Sulfur Dioxide through Polymer Membranes. 1. Polyacrylate and Cellulose Triacetate Single-Layer Membranes, Ind Eng Chem Proc Dd, 19 (1980) 609-616.
[38] D.L. Kuehne, S.K. Friedlander, Selective Transport of Sulfur-Dioxide through Polymer Membranes .2. Cellulose Triacetate-Polyacrylate Composite Membranes, Ind Eng Chem Proc Dd, 19 (1980) 616-623.
[39] R.M. Felder, R.D. Spence, J.K. Ferrell, Permeation of sulfur dioxide through polymers, Journal of Chemical & Engineering Data, 20 (1975) 235-242.